Crystallization of Ultrathin Films of Polylactides: From Chain Chirality to Lamella Curvature and Twisting

Damien Maillard and Robert E. Prud'homme*

Département de Chimie, Université de Montréal, Succursale Centre-Ville, C.P. 6128, H3C 3J7 Montréal, Québec, Canada

Received June 12, 2007; Revised Manuscript Received December 14, 2007

ABSTRACT: The crystallization of poly(D-lactide) (PDLA) and poly(L-lactide) (PLLA) in ultrathin films (15 nm) has been followed between 125 and 160 °C using *in situ* atomic force microscopy. Using a forced nucleation technique, edge-on lamellae were observed, showing a curvature which is related to the polymer chirality. In the case of PLLA, the lamellae are S-shaped, contrary to the PDLA lamellae which are Z-shaped. This behavior was also observed on TEM pictures of PLLA and PDLA films crystallized in the same conditions, without any external nucleation. As shown by electron diffraction patterns, the crystalline unit cells of the two enantiomers are identical. For the first time, a relationship has been established between the molecular chirality of poly(lactide)s and their macroscopic behavior. Moreover, the direction of curvature of the lamellae can be linked with the sense of twisting of the poly(lactide) lamellae in banded spherulites, and the temperature dependence of the radius of curvature can be correlated with the distance between the extinction rings. Those observations are consistent with Keith and Padden's model since the curved crystals in ultrathin films can be considered as "half-lamellae", which give, when associated together, twisted complete lamellae.

Introduction

From Pasteur until today, the link between molecular chirality and crystalline morphology has intrigued scientists.[1] If a correlation in the case of small molecules is now well established, in which a dissymmetric behavior of crystals is a common feature, macromolecules represent a greater challenge. The diversity of macromolecular architectures and crystalline morphologies and the particular arrangement of the chains inside the lamellae are some of the factors that contribute to make this case more elusive.

In polymers, the most notorious example is the observation of twisted lamellae in polyethylene spherulites, which is not a chiral polymer, conducting to extinction rings. For chiral polymers, the best example is that of poly(epichlorohydrin) in which the rotational sense of lamellar twisting in spherulites has been correlated with the main-chain chirality,[2−4] i.e., the right-handed polymer gives a crystallite rotating clockwise, and the left-handed polymer gives a crystallite rotating counterclockwise.

The origin of lamellar twisting has been the subject of several studies, and two main explanations are generally considered. In the first one, Bassett et al. proposed that the twists result from the sum of isochiral screw dislocations.[5] However, Xu et al., for example, observed in real time the onset of twisting before the appearance of any screw dislocation,[6] and therefore, this explanation is often challenged. In the second explanation, Keith and Padden proposed that the phenomenon is due to an unbalanced surface stress repartition.[7,8] The lamella can be described as made of two welded half-lamellae, each one trying to scroll in an opposite direction, leading to a complete twisted lamella. The scrolling of the half-lamella is due to a surface stress difference between the two fold surfaces caused by different factors like the chain tilting in the case of polyethylene,[7] the chemical structure of the chain folds in the case of polyamide 66,[9] or the main-chain chirality in the case of biopolymers.[10]

In a previous communication,[11] we have shown that, in ultrathin films of poly(lactide)s, a chiral polyester, different morphologies are observed for the two enantiomers. The edge-on lamellae are S-shaped in the case of poly(L-lactide) (PLLA) but Z-shaped in the case of poly(D-lactide) (PDLA). If the edge-on lamellae are identified as Keith and Padden's half-lamellae, the same sort of curvature, different for PDLA and PLLA, is expected in lamellae crystallized in the bulk, in the form of twisted lamellae conducting to banded spherulites. It is one of the purposes of this paper to verify this hypothesis. We will also show that the curvature observed in ultrathin films by atomic force microscopy (AFM), after a forced nucleation, can also be seen by transmission electron microscopy (TEM) on ultrathin film and by polarized optical microscopy (POM) on thick samples, without resorting to a forced nucleation.

Poly(lactides) are biodegradable and biocompatible polyesters synthesized via ring-opening polymerization from renewable carbon sources.[12] The repeat unit of the polymer contains an asymmetric carbon: the D and L enantiomeric forms, containing respectively only R or S asymmetric carbon atoms, are semicrystalline and exhibit three different crystalline states. The α phase, observed from solution and melt crystallization, is the most common, whereas the β and γ phases are generated from extrusion or stretching.[13] The crystalline unit cell of the α phase is pseudo-orthorhombic with parameters $a = 1.07$, $b = 0.62$, and $c = 2.88$ nm, and the chains are arranged in a 10_3 helical conformation.[14] The helix is left-handed in the case of PLLA and right-handed in the case of PDLA.

Experimental Part

Materials. Poly(L-lactide) was provided from Polysciences Inc. and poly(D-lactide) from Purac Inc.; both were used without further purification. Their molecular weights were determined by gel permeation chromatography using a Wyatt light scattering detector: $M_n = 120\,000$ g mol^{-1} and polydispersity (PD) = 1.30 for the poly(D-lactide); $M_n = 110\,000$ g mol^{-1} and PD = 1.26 for the poly(L-lactide). Glass transition temperatures and melting points were determined using a Perkin-Elmer DSC-7 apparatus. For PLLA,

* Corresponding author. E-mail: re.prudhomme@umontreal.ca.

10.1021/ma071306u CCC: $40.75
Published on Web 02/08/2008

T_g = 57 °C and T_f (maximum of the peak) = 176 °C; for PDLA, T_g = 56 °C and T_f (maximum of the peak) = 180 °C. Poly(ethylene glycol) was provided from Aldrich Chemical Co. (M_v = 100 000 g/mol) and used without further purification.

Sample Preparation. Ultrathin films were prepared by spin-coating at a rotation speed of 3000 rpm for 20 s, following an acceleration of 4000 rpm/s, using a Headway Research Inc. EC-101 apparatus. Dichloromethane was used as solvent. The film thickness was controlled by the solution concentration; concentrations from 1 up to 20 mg/mL can be used to obtain thicknesses ranging between 5 and 100 nm. The thickness of 15 nm was obtained with concentration of 3 mg/mL. The films were cast onto cleaned Si substrates (p-type single side polished (100) silicon wafers) for the AFM observation. The wafers were cleaned by immersion in nitrohydrochloric acid for 1 h in an ultrasonic bath to remove any organic contamination and to hydroxylate the native oxide layer, thus making the surface hydrophilic. The substrates were then rinsed with distilled water and dried by spin-coating for 40 s at 3000 rpm, before treatment in a plasma cleaner (Harrick PDC-32G) at 18 W for 20 s. To keep a solvent-saturated atmosphere around the sample and to allow a uniform evaporation, a glass dome was placed on top of the sample area during spin-coating. Film thicknesses were measured by atomic force microscopy. In the case of TEM observations, ultrathin films were spin-coated on freshly cleaved mica covered by a carbon layer (108 carbon/A, Cressington Carbon Coater).

Thick films were prepared by solvent evaporation in dichloromethane on microscope glass slides. The thickness of the film was controlled by the concentration of the solution.

Atomic Force Microscopy. A Nanoscope III Multimode AFM apparatus (Digital Instrument (DI)), operated in tapping mode and equipped with a high-temperature heating accessory (DI), was used to capture images. A JVH scanner was used (maximal scan size 130 × 130 μm) with silicon nitride probes (MikroMasch and Nanosensor).

Spin-coated samples, previously fractionated into small square areas and glued onto steel pucks, were melted in the AFM stage at 185 °C for 2 min. Then, the stage temperature was decreased to the chosen crystallization temperature (between 110 and 165 °C). The surface was observed with a scan size of 50 × 50 μm and zoomed to observe more accurately some details. During the whole process, the AFM probe was maintained at the same temperature as the sample to avoid any condensation. The scan rate was 1 Hz. Nucleation was induced by decreasing suddenly the AFM probe amplitude set point along one line to initiate a contact. Height, amplitude, and phase were collected simultaneously. Each sample was used only once, at one temperature. Edge-on lamellar densities were obtained by counting the number of lamellae enumerated along the nucleation line and dividing by the length of this line; averages of three repetitive experiments are reported. The radii of curvature were measured with the Image-Pro Plus 5.1 software by tracing a circle along the curvature of the observed lamellae. The radii reported in this study are the average of between 25 and 40 measurements, depending on the crystallization temperature (increasing the temperature decreases the number of observed lamellae).

Transmission Electron Microscopy (TEM). A JEOL JEM-2010 transmission electron microscope operating at 80 kV was used for the TEM and electron diffraction experiments. The films were melted 10 min at 185 °C and crystallized on mica at the desired temperature in a THMS-600 Linkam hot stage connected to a TMS 94 temperature controller. After crystallization, samples (on mica) were placed on an aluminum sheet previously cooled in liquid nitrogen, quickly decreasing the temperature below the glass transition and freezing the sample. The films were separated from the mica by floating them in water, and they were transferred on copper grids for observation.

Polarized Optical Microscopy (POM). An Axioskop 2 and an Axioskop 40 from Carl Zeiss, equipped for polarized microscopy, were used to observe thick films. The films (10 μm thick, obtained from solvent casting) were melted at 185 °C between two glass slides for 10 min in a THMS-600 Linkam hot stage connected to a TMS-94 temperature controller. The temperature was decreased slowly (0.5 °C/min) at 160 °C and maintained for 1 h. Then, the temperature was slowly decreased to the chosen crystallization temperature (between 110 and 150 °C). Pictures were taken with a Micropublisher 3.3 camera from Q-Imaging and analyzed with the Image-Pro Plus 5.1 software. The rotation experiments were done with a custom-made goniometer installed on the microscope stage. The samples were observed during a rotation around the *Y*-axis, and the position of the extinction rings was followed. During those experiments, the two polarizers were tilted at respectively −45° and 45° of the *Y*-axis, permitting an observation at 45° of the maltese cross extinction area.

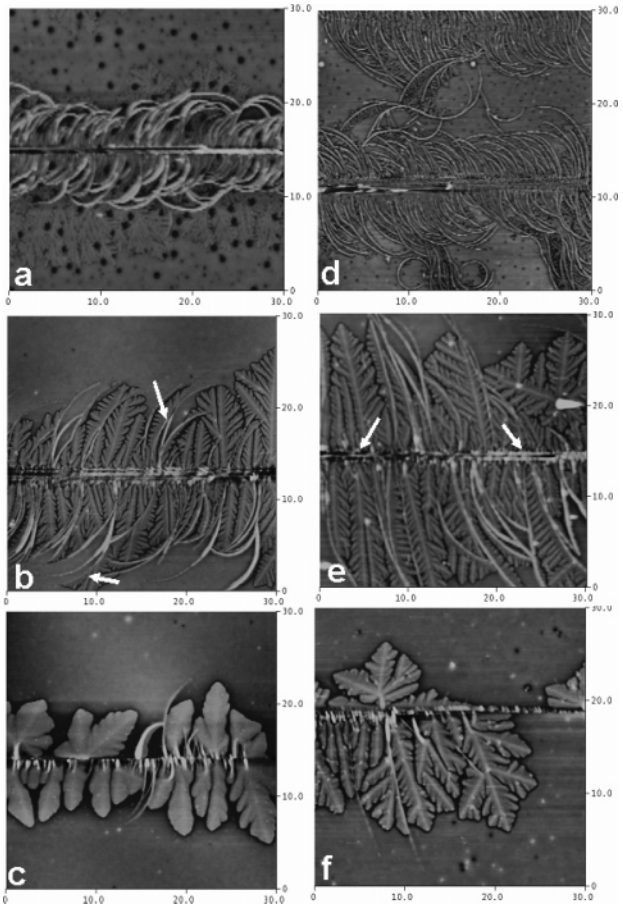

Figure 1. AFM pictures of ultrathin films (30 × 30 μm) of PLLA (a, b, c) and PDLA (d, e, f), all 15 nm thick and crystallized via the forced nucleation technique. (a) and (d) were crystallized at 125 °C, (b) and (e) at 145 °C, and (c) and (f) at 160 °C.

Results and Discussion

1. Edge-On Behavior.

1.1. AFM Observations. In a short communication, we have recently shown that, following a forced nucleation with an AFM tip, ultrathin films of poly(D-lactide) and poly(L-lactide) behave differently.[11] In both cases, the contact between the tip and the melted sample creates a chain alignment parallel to the substrate conducting to edge-on lamellae (surrounded by a sea of flat-on lamellae), and the lamellae are curved, as it is normally the case in the literature.[15] However, the sense of curvature is different for PLLA and for PDLA. In the first case, the edge-on lamellae exhibit a S-shape, whereas in the second one, they show a Z-shape.

Figure 1 shows AFM pictures of several 15 nm thick films of PLLA (Figures 1a−c) and PDLA (Figures 1d−f) crystallized at specific temperatures (125 °C for Figures 1a,d, 145 °C for

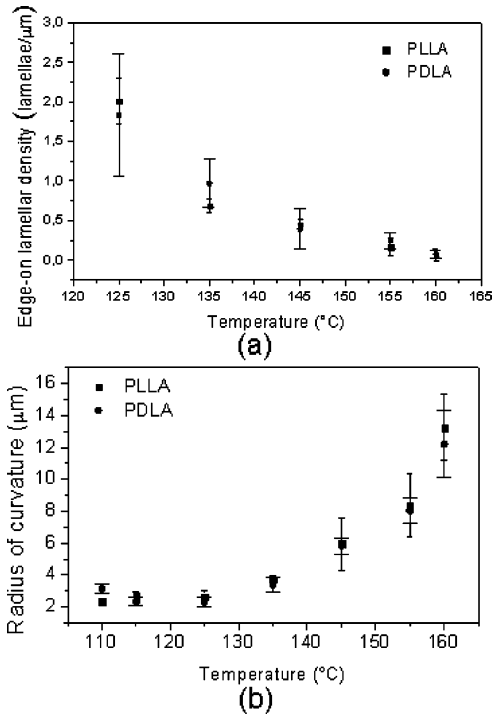

Figure 2. Variation of (a) the density of edge-on lamellae and (b) the radius of curvature vs the crystallization temperature for 15 nm thick PDLA and PLLA films.

Figures 1b,e, and 160 °C for Figures 1c,f). In each case the crystallization was nucleated by a contact line between the film and the AFM tip which can be seen at the center of each picture, with the formation of edge-on lamellae surrounded by flat-on lamellae.

For this film thickness (15 nm) and range of crystallization temperatures (from 125 to 160 °C), the flat-on lamellae are systematically dendritic. They are, in some cases, nucleated directly by the contact line (arrows in Figure 1e) or, in others, by the edge-on lamellae (arrows in Figure 1b). At 125 °C (Figures 1a,d), the lamellar thickness is close to the film thickness and, therefore, the contrast on the AFM height image is poor. Since the lamellar thickness increases with the temperature, the contrast also increases from 125 to 160 °C (Figure 1a vs Figure 1c).

The edge-on lamellae are nucleated directly from the contact line and grow perpendicularly to that line. They quickly exhibit a curved shape, and the sense of the curvature depends only on the chain chirality, S-shaped for the PLLA (Figures 1a−c) and Z-shaped for PDLA (Figures 1d−f).

The density of edge-on lamellae decreases with the temperature, as seen qualitatively in Figure 1 and quantitatively in Figure 2a. This is a well-known effect predicted by all nucleation theories:[16,17] nucleation is more efficient at low temperatures than at high temperatures.

The radius of curvature increases with the temperature, as seen in Figures 1 and 2b. Below 130 °C, the high nucleation density forces the lamellae to grow perpendicular to the nucleation line, conducting to close-packed structures from which grow the flat-on lamellae (Figures 1a,d). Because of the combined effect of high nucleation density and small radii of curvature, the zone surrounding the nucleation line in which edge-on lamellae grow is thin and is continued by flat-on lamellae (Figure 1a). At temperatures higher than 130 °C, the lamellae have more lateral freedom, due to the lower nucleation density, until they become "strangled" by the flat-on lamellae.

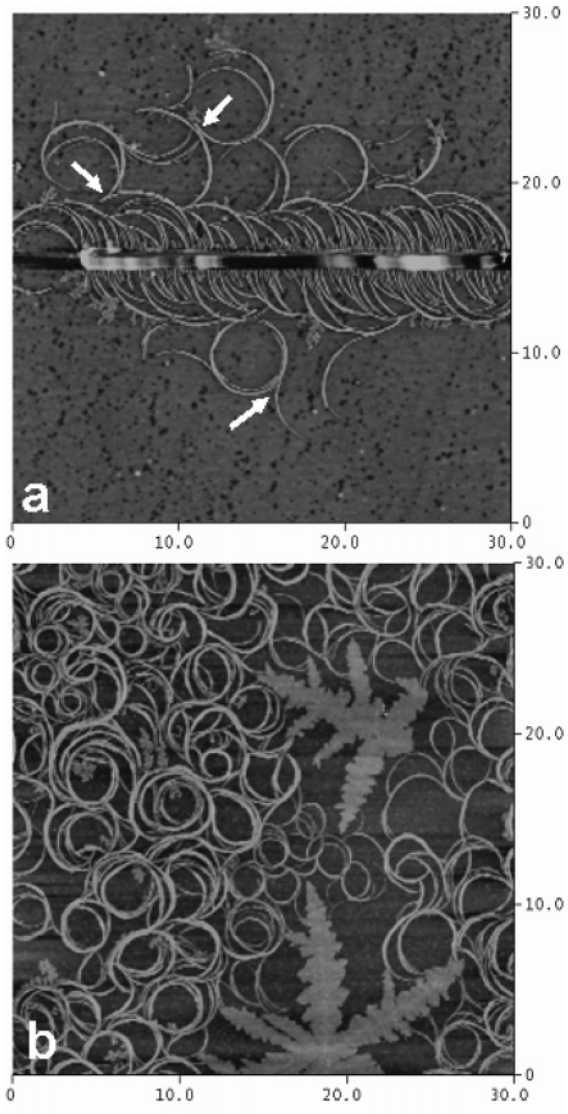

Figure 3. AFM pictures of ultrathin films (thickness = 8 nm) of PDLA: (a) crystallization at 125 °C *in situ* with induced nucleation and (b) crystallization for 15 h in a hot stage before quenching in liquid nitrogen. In the second picture, edge-on lamellae, in the form of loops, compete with flat-on lamellae, in the form of snowflakes.

At very low film thicknesses, 10 nm and less, and at a crystallization temperature of 125 °C, edge-on lamellae act as secondary nuclei to other edge-on lamellae, as illustrated in Figure 3, leading to U-shape and loop-shape lamellae. As shown in Figure 3a, the second generation of lamellae grows tangentially to the first generation, in the opposite direction, but with the same curvature behavior (see the arrow): they always turn to the left for PDLA and to the right for PLLA. This behavior was observed in the case of induced nucleation (Figure 3a), but also for samples crystallized outside the AFM and observed at ambient temperature (Figure 3b).

Two questions arise from these observations. Is the existence of edge-on lamellae due mainly to the forced nucleation? And, is the direction of curvature driven by the tip movement? To answer these questions, other techniques must be used.

1.2. TEM Observations. TEM observations were done for two different purposes. First, TEM was used to perform electron diffraction experiments that permitted to obtain the *a* and *b* crystalline unit cell parameters for each of the two enantiomers. Second, TEM was also used to support and validate the AFM observations. In the AFM technique, the contact between the

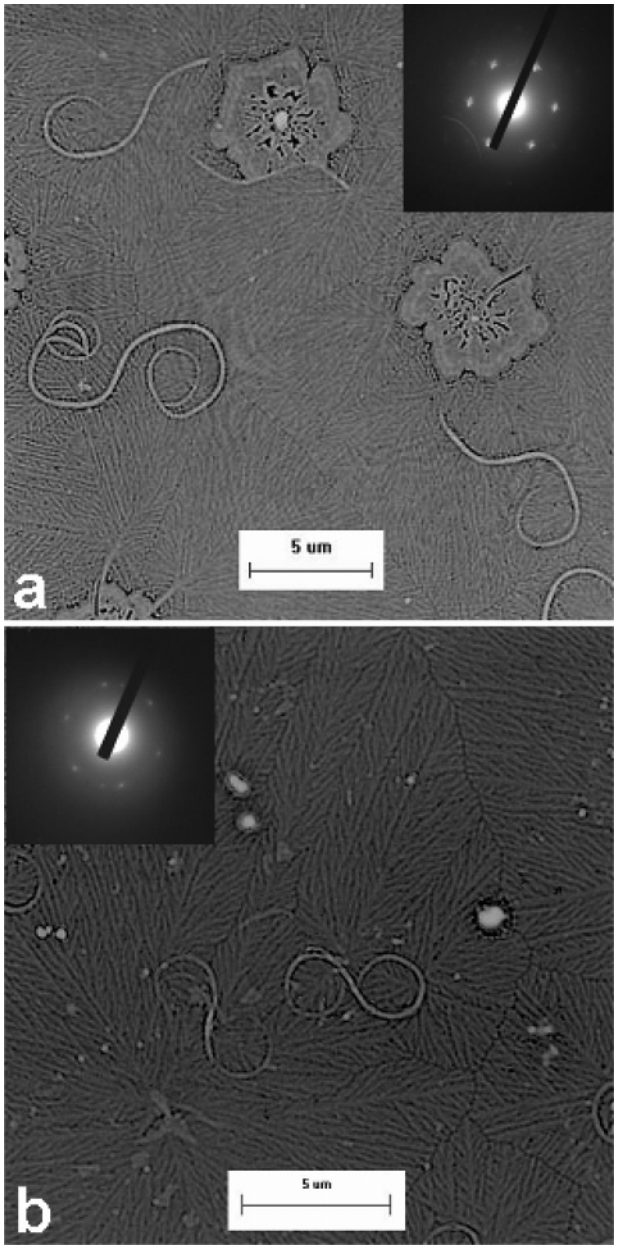

Figure 4. TEM pictures of (a) PLLA and (b) PDLA films of 15 nm thickness crystallized at 125 °C. The corresponding electron diffraction patterns are shown; in both cases, the measured *ab* angle of the unit cell is 90°.

sample and the probe could possibly induce artifacts, especially in the case of melt crystallization. For the TEM observations, the samples were isothermally crystallized in a confined stage before freezing in liquid nitrogen, and they were observed without any contact with a probe.

Figure 4 shows pictures obtained for the two polylactide enantiomers, for samples crystallized at 125 °C for 24 h at film thickness of 15 nm. The two pictures are very similar: the complete surface of the film is covered by dendritic flat-on lamellae, and in some instances, edge-on lamellae are visible. Those lamellae are, again, curved with a characteristic orientation, a S-shape for PLLA and a Z-shape for PDLA. Electron diffraction patterns corresponding to the flat-on crystals are given for each picture. Using those patterns, *a* and *b* crystalline cell parameters were calculated: $a = 1.12$ and $b = 0.64$ nm for PLLA, and $a = 1.10$ and $b = 0.63$ nm for PDLA. Those parameters are close to those reported in the literature for polylactide.[14,18] The *ab* angle is 90°.

Similar experiments were done for a broad range of temperatures, from 120 to 160 °C, and the same behavior was observed in all cases, with isolated curved edge-on lamellae surrounded by flat-on lamellae; at each temperature, for thicknesses ranging from 10 to 50 nm, edge-on lamellae are present. As in the AFM observations, the edge-on lamellae show a specific curvature only driven by the chirality of the chain: S and Z shapes characteristic of PLLA and PDLA, respectively. These lamellae, spontaneously nucleated, are able to scroll (Figure 3a) or to adopt an "eight" shape (Figure 3b).

From the literature, the *ab* angle measured for PLLA and PDLA is 90°, verifying the orthorhombic symmetry of the crystalline unit cell; the *ab* angle measured herein using electron diffraction is also 90°. The absence of deformation of the electron diffraction pattern confirms that the electron beam is naturally aligned along the *c*-axis. As the beam presents no tilt and the sample is oriented perpendicularly to the beam, the *ac* and *bc* angles are 90°. The crystal symmetry is definitely orthorhombic, and the curvature is not due to the presence of tilt. In view of this observation, it can be concluded that the origin of the curvature does not come from the crystalline structure, but probably from the amorphous chain folds at the crystal surface.

1.3. POM Observations. In the second part of this study, thick polymer films (10 μm) made of 75% polylactide (L or D) and 25% poly(ethylene glycol) (PEG) have been observed using optical microscopy. Before crystallization, those films were prepared by solvent evaporation (dichloromethane) at ambient temperature. During the solvent evaporation, crystallization occurs (there is no trace of crystallization of PEG under those conditions) in a very unusual way, as exemplified by the pictures shown in Figure 5.

A similar behavior can be observed on both Figure 5a (75/25 PLLA/PEG) and Figure 5b (75/25 PDLA/PEG): the presence of crystalline star-shaped structures. Those structures are made of edge-on lamellae radiating from a central point, looking like spherulites in an early stage of growth. The lamellae are curved, with the same specific sense of curvature than seen in the previous sections: S-shaped for PLLA and Z-shaped for PDLA. The dark dots on the pictures are PEG clusters rejected from the polylactide phase. Their size, of about 1 μm, seems to be independent of the amount of PEG used.

The edge-on lamellae, and their chiral specificity, are thus not restricted to ultrathin films. Those lamellae, aligned side by side in AFM observations, or isolated in TEM observations, can also be observed with optical microscopy organized in star-shaped structures.

2. Lamellar Twisting in Spherulites. The previous examples were limited to isolated edge-on lamellae. For a broader view of all aspects of this phenomenon, especially in the bulk, the case of spherulites was also investigated.

The most common manifestation of the presence of lamellar curvature in spherulites is the observation of extinction rings. Those rings are indicative of lamellar twisting inside the spherulites. Polymers like polyethylene, which have no molecular chirality, exhibit lamellar twisting. For chiral polymers, like poly(epichlorohydrin) (PECH) or poly(3-hydroxybutyrate), extinction rings are usually observed in the spherulites, and for PECH, the sense of twisting has been correlated to the chirality of the chain.[2] However, no generalization can be made since this observation is not true for poly(3-hydroxyvalerate) and poly(3-hydroxybutyrate), which both exhibit a left-handed chain helix, but they lead to right-handed and left-handed lamellar twisting, respectively.[4]

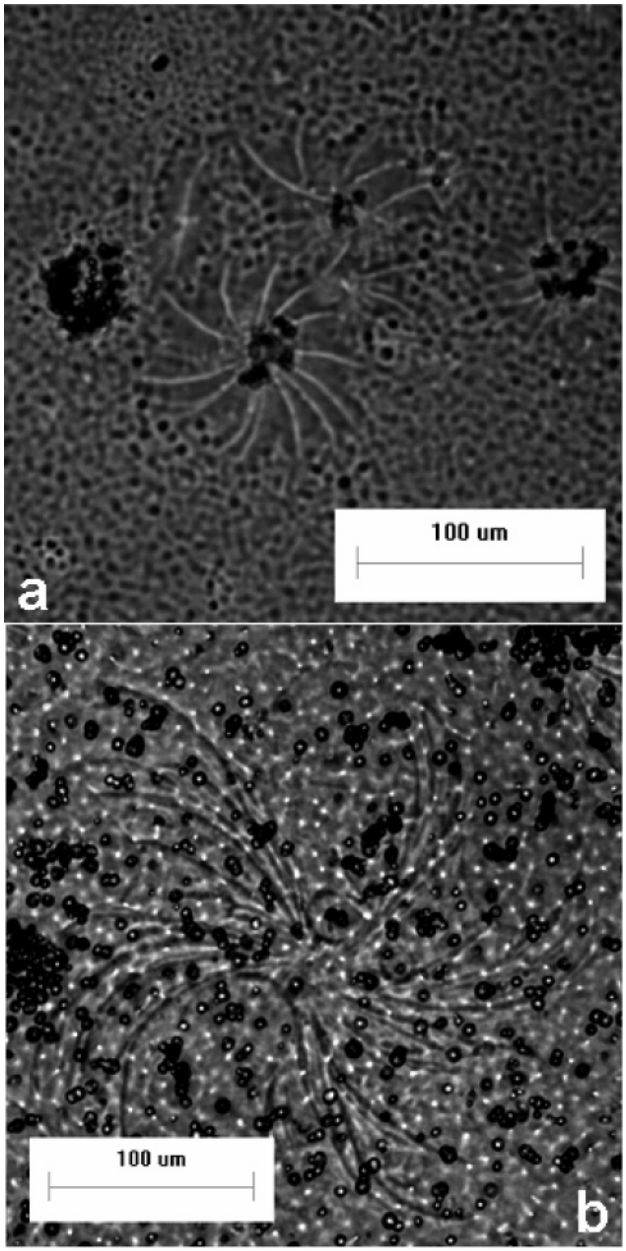

Figure 5. Polarized microscopy pictures of 10 μm thick polymer blend films composed of 25% of PEG and 75% of (a) PLLA or (b) PDLA. The films were prepared by solvent evaporation from dichloromethane solutions and were kept at ambient temperature.

Poly(lactide) spherulites are generally not banded, but under conditions described by Xu et al.,[19] extinctions rings can be obtained. In pure PLLA or PDLA, the extinction rings only appear in a narrow range of temperatures, actually too narrow to be considered in the present study. However, the addition of poly(DL-lactide) or poly(hydroxybutyrate) to poly(L-lactide) is known to induce the presence of extinction rings and to decrease the band spacing, expanding the range of temperatures with extinction rings.[19] Recent studies conducted in our group have shown that poly(ethylene glycol) also has the capacity to "stimulate" the twisting of PLLA,[20] and for this reason, that additive was chosen in the present work. Figure 6a exhibits a PLLA film melted 10 min at 185 °C and quickly cooled (50 °C/min) to 120 °C. Spherulites are clearly visible, but they exhibit no extinction rings. However, Figure 6d exhibits a PLLA film containing 25% of PEG crystallized at 120 °C, after a rest at 160 °C for 1 h; the spherulites exhibit clear extinction rings.

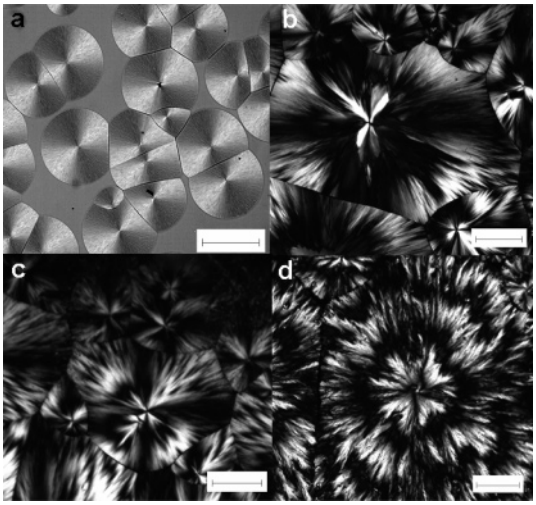

Figure 6. (a) Polarized optical microscopy pictures of 10 μm thick films of pure PLLA crystallized at 120 °C after melting at 185 °C for 10 min (cooling rate of 50 °C/min). (b, c, d) Polarized optical microscopy pictures of 10 μm thick films of (b) 90/10, (c) 85/15, and (d) 75/25 PLLA/PEG mixtures, crystallized at 120 °C after melting at 185 °C for 10 min (decrease of 50 °C/min) and a rest at 160 °C for 1 h (cooling rate of 0.5 °C/min). Scale bars length is 200 μm.

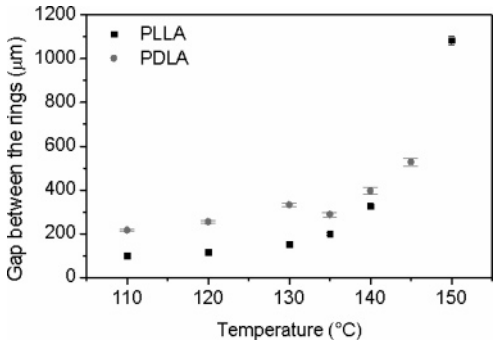

Figure 7. Distance between the extinction rings as a function of crystallization temperature in thick films of PLA and PEG blends (75% PLA and 25% PEG).

Figures 6b,c show PLLA films crystallized with the same thermal treatment but with a smaller quantity of PEG (10 and 15%, respectively). The extinction rings are not as well-defined as in Figure 6d.

Figure 7 shows the effect of temperature on the distance or gap between the extinction rings of 75/25 PLLA/PEG blends which increases quasi-exponentially with the temperature, in agreement with the literature.[19] This observation can be compared with the increase of the radius of curvature of half-lamellae with temperature (Figure 2b). However, it does not provide any information on the direction of the twist.

The sense of twisting of the lamellae inside the spherulites was determined using polarized microscopy. The optic axis of crystalline poly(lactide) is along the chain. In the case of twisted lamellae oriented radially in the spherulite (the chain *b*-axis is radial), the optic axis (*c*-axis) changes its orientation along the lamella, according to the twist, alternatively perpendicular and parallel to the incident polarized light. This alternation leads to extinction rings.

By analogy between a twisted lamella and a screw, since a right-handed positive rotation applied to a right-handed screw conducts to a visual descent of the apparent screw thread, a twisted lamella rotated in the sense of its own twist leads to a descent of the corresponding extinction rings. The opposite effect is also observed; i.e., a right-handed positive rotation of

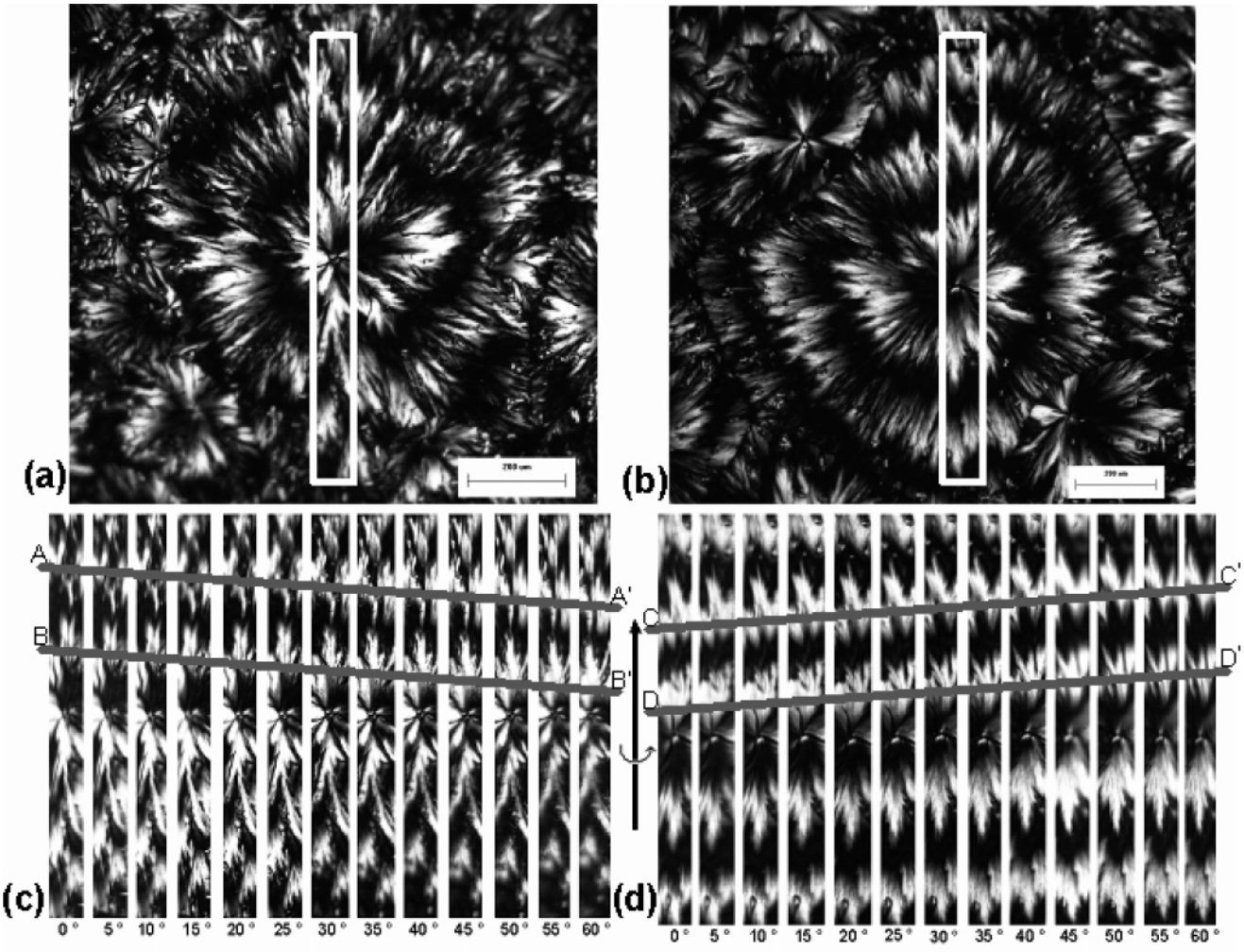

Figure 8. Spherulites of (a) PLLA and (b) PDLA of 10 μm thick 75/25 poly(lactide)/poly(ethylene glycol) films crystallized at 120 °C after having been maintained 1 h at 160 °C. The delimited area in (a) and (b) represents the observed slice during the rotation experiment. Vertical sections of (c) PLLA and (d) PDLA spherulites observed during the rotation by polarized optical microscopy with a 10× objective. The values at the bottom represent the angle of twist around the *Y*-axis in the right-handed positive sense. Scale bars length is 200 micrometers.

a left-handed screw leads to a visual raise of the apparent screw thread and, accordingly, in the case of lamellae, to a raise of the corresponding extinction rings.

Therefore, it is possible, using polarized optical microscopy, to determine the sense of twisting of a lamella inside a spherulite. To achieve that, a goniometer was introduced in the microscope stage to hold the sample, and the sample was rotated along the *Y*-axis (the light crossing the sample along the *Z*-axis). By applying a right-handed rotation on the PLA samples and observing the shift of the extinction rings for the two enantiomers, it was possible to determine the sense of twisting of the lamellae.

Figure 8 shows polarized microscopy pictures of the central vertical slice of PLLA and PDLA spherulites subjected to a right-handed rotation. In the case of PLLA (Figure 8c), a descent of the extinction rings is clearly seen, underlined with the AA′ and BB′ lines. A descent of the extinction rings means that the screw goes in the same sense than the applied rotation. In that case, the twisted lamella appears to be right-handed. In contrast, in the case of PDLA (Figure 8d), the inverse behavior is observed, underlined with the CC′ and DD′ lines. In that case, the sense of twisting of the lamella is opposite to the sense of rotation. The lamella is left-handed.

Discussion

In this paper, we have observed S-shaped and Z-shaped edge-on lamellae for PLLA and PDLA, respectively, not only for ultrathin samples crystallized after inducing the nucleation with an AFM tip but also for samples crystallized in an isolated environment (TEM observations) and for thick samples crystallized in the melt (POM observations). In the last case, most lamellae are surrounded by other polylactide chains and do not lie on a substrate. These lamellae were observed over a broad range of temperatures, from 110 to 165 °C (pictures in this article cover the 125−160 °C range).

In the context of Keith and Padden's theory, in which a lamella can be described as made of two welded half-lamellae, the nucleation and growth of edge-on lamellae in ultrathin films are limited in space due to the presence of the substrate. During their early stage of growth, edge-on lamellae are similar to flat-on lamellae, but quickly, an edge of the lamella meets the substrate. According to Doi et al., the *b*-axis of the lamella is oriented parallel to the substrate, and since the crystalline cell is orthorhombic, the *a*-axis is perpendicular to the substrate. The (200) growth fronts of the crystal are quickly stopped in their development: the inferior front reaches the substrate and stops there, while the superior front emerges from the melt. (According to AFM measurements, edge-on lamellae emerge

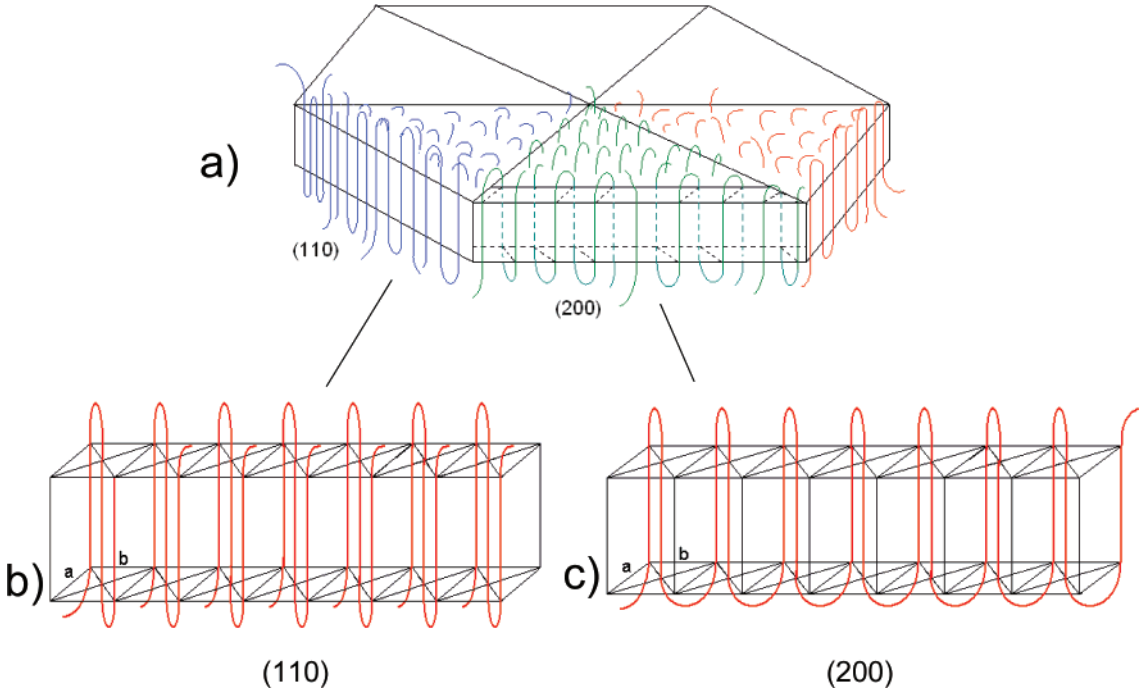

Figure 9. Chain arrangement in the crystal with (200) and (110) sectors. In the first case, the folding occurs in zigzag, contrary to the second case where the chains follow a straight line.

about 35 nm above the melt in ultrathin films having a thickness inferior to 20 nm.) As the superior growth front is able to go through the molten polymer−air interface and to emerge from it (the lamella height is larger than the film thickness), contrary to the inferior growth front which is suddenly stopped by the molten polymer−substrate interface, the resultant lamella is not symmetric and its inferior part is atrophied in comparison with its superior part. This lamella can be considered as a "half-lamella".

The crystal grows freely along the *b*-axis, in two directions, adopting a ribbon or snake shape (Figures 1a,b). This half-lamella scrolls on itself adopting a final S or Z shape, probably for surface chain folding reasons. In the case of thick films, the lamellae do not scroll but twist. The Keith and Padden theory states that the twist of a lamella results from the tendency for scrolling in opposite directions of the two "half-lamellae". According to that theory, the result of the appearance of scrolled instead of twisted lamellae is the atrophy of one of the half-lamellae. It is therefore concluded that the "phantom half-lamella" (the atrophied one) has a sense of curvature opposite to the superior half-lamella. (At the beginning, the two-half-lamellae are equivalent, but the phantom lamella is inverted, as compared to the superior lamella.) And, finally, knowing the sense of scrolling of the superior lamella (which is not atrophied since it can emerge in air from the melt), it is possible to deduce the sense of twisting of the corresponding complete lamella.

In the case of PLLA, since the superior half-lamella is S-shaped and the phantom inverted lamella is Z-shaped, the resultant total lamella (in spherulites) needs to be twisted right-handed. Conversely, in the case of PDLA, the superior half-lamella is Z-shaped, the phantom inferior lamella S-shaped, leading to a left-handed twisted lamella. The observations made in the previous section of this paper, with S or Z-shaped lamellae in thin films, translating, respectively, in right-handed or left-handed twisted lamellae in spherulites, are consistent with this explanation. Therefore, the twisting of the lamellae inside the spherulites finds its source in the scrolling of the two half-lamellae.

In other words, the twisting of the lamellae in banded spherulites is an intrinsic property of the material, resulting from the chain chirality; it is left-handed in PDLA and right-handed in PLLA. However, when the film thickness goes down to nanometer dimensions, for edge-on lamellae, the two half-lamellae cannot develop freely, as they do in the bulk. The substrate stops the growth of the half-lamella in its vicinity whereas the other half-lamella continues to grow on the air side (because it can emerge from the melt). Under these conditions, the left-handed helix of PDLA necessarily gives a Z-shaped edge-on lamella whereas the right-handed helix of PLLA necessarily gives a S-shaped edge-on lamella—the same shape would be observed if the growth would occur on the ceiling of a space shuttle in the absence of gravity.

This brings us to the question of knowing how does the chirality impact on the folding organization? One important observation is that the temperature influences the spherulites and edge-on lamellae; i.e., upon decreasing the temperature, both the radius of curvature of edge-on lamellae and the band spacing of the spherulites are reduced. This observation can be correlated with the crystal thickness which increases with the temperature. Actually, the thickness of the folded chain layer at the surface of the crystal is constant, but the thickness of the crystalline section increases with temperature. Therefore, the percentage of folded chain in the crystal decreases with the temperature.

The chain folding applies a force on the crystalline phase, and the resultant deformation depends on the capacity of that crystalline phase to resist. The thicker the crystalline phase, the smaller the deformation of the lamella due to the chain folding. As the fraction of chain folding phase decreases with temperature, the band spacing in banded spherulites and the radius of curvature in edge-on lamellae increase with a raise of the temperature.

A poly(lactide) crystal is divided into six sectors, two (200) and four (110) sectors. In the (110) sectors, the chain folds are parallel to the growth front (Figure 9b); i.e., the chains are (110) oriented. In the (200) sectors, the chain folds are successively aligned along the (110) and the (1−10) axes. The folded chains

are never aligned along the *a*-axis the *b*-axis, but always in diagonal. In the (200) sectors, as shown in Figure 9c, the chain folding is oriented differently on the two sides of the lamella.[21] This difference between the two sides of the lamella could be at the origin of the unbalanced surface stress conducting to the scrolling.

Another possible origin for the unbalanced surface stress could be the exit angle of the chain from the lamella. Because of the helical conformation of the chain and the symmetry of the crystalline cell, the chain exits from the lamella with a specific angle which is always the same on the face of a (110) sector and opposite on the other face. The resulting pressure applied by the small fraction of the chain in contact with the crystal could lead to a curvature. The exit angle is linked to the sense of rotation of the chain helix. Inverting the chain helix should invert the exit angle and the sense of curvature of the half-lamella.

In summary, we found by AFM, TEM, and POM that there is a chirality transfer in polylactides from the chain structure (chiral centers) to the macroscopic level (lamella curvature), at different length scales in a hierarchical order. The chirality transfer follows specific steps which can be decomposed as follows: transfer of the chain chirality to the sense of rotation of the helix; transfer from the helix to the chain folding organization on the surface of the lamella, giving rise to the half-lamella curvature, as observed in Figures 1, 4, and 5 coming from AFM, TEM, and POM microscopies, respectively; and, finally, transfer from the half-lamella to the complete twisting of the lamella in the spherulites, as observed in Figure 8 by POM measurements. These are the four levels that have been described by Li et al.:[22] configurational, conformational, lamellar, and spherulitic.

This sort of transfer is common in small molecules[23,24] and biological macromolecules,[10] although the intrinsic reasons for having different orientations of the two enantiomers can be very different from one case to another, especially if small molecules and macromolecules are compared. However, in the literature, the cases of poly(epichlorohydrin)[3] or series of chiral polyesters[25−27] can be compared with that of polylactides. In poly(epichlorohydrin), the link between the lamellar twist, which conducts to the banding of the spherulites, and the polymer chirality has been clearly established, but it was not possible to extend the observation to the monocrystal level, although the chirality was clearly at the origin of lamellar twisting and twisting direction. In the present paper, the influence of chirality on the crystallization of a synthetic polymer at the quasi-monocrystal level (lamellae in ultrathin films) and on the twisting of lamellae in spherulites has been simultaneously observed for the first time.

Can we expect the same behavior for all chiral polymers? The literature indicates that the chirality of the repeat unit is not the only factor contributing to the control of the morphology. For example, Li et al.[22] have shown that main-chain chiral liquid crystals (CLC) transfer their chirality to the level of chiral helical single crystals, which are right-handed with right-handed CLC but left-handed with left-handed CLC. However, adding a single methylene unit to the CLC leads to an inversion of the handedness of the helical crystals; i.e., the right-handed CLC leads to left-handed helical crystals. Similarly, poly(3-hydroxyvalerate) and poly(3-hydroxybutyrate) both exhibit a left-handed chain helical conformation, but they lead to right- and left-handed lamellar twisting, respectively.[4] These two examples clearly show that the chiral center at the configurational level is not the only factor controlling the handedness of the crystal.

Acknowledgment. The authors thank the Natural and Engineering Research Council of Canada (NSERC) and the Department of Education of the Province of Québec (FQRNT program) for financial support. We also gratefully acknowledge PURAC America Inc. for providing PDLA for this research.

References and Notes

(1) Pasteur, L. *Ann. Chim. Phys.* **1848**, *24*, 442−459.
(2) Singfield, K. L.; Brown, G. R. *Macromolecules* **1995**, *28*, 1290−1297.
(3) Singfield, K. L.; Klass, J. M.; Brown, G. R. *Macromolecules* **1995**, *28*, 8006−8015.
(4) Saracovan, I.; Cox, J. K.; Revol, J. F.; Manley, R. S. J.; Brown, G. R. *Macromolecules* **1999**, *32*, 717−725.
(5) Bassett, D. C.; Hodge, A. M. *Polymer* **1978**, *19*, 469−472.
(6) Xu, J.; Guo, B.; Zhang, Z.; Zhou, J.; Jiang, Y.; Yan, S.; Li, L.; Wu, Q.; Chen, G.; Schultz, J. M. *Macromolecules* **2004**, *37*, 4118−4123.
(7) Keith, H. D.; Padden, F. J. *Polymer* **1984**, *25*, 28−42.
(8) Keith, H. D.; Padden, F. J. *Macromolecules* **1996**, *29*, 7776−7786.
(9) Cai, W.; Li, C. Y.; Li, L.; Lotz, B.; Keating, M.; Marks, D. *Adv. Mater.* **2004**, *16*, 600−605.
(10) Lotz, B.; Gonthier-Vassal, A.; Brack, A.; Magoshi, J. *J. Mol. Biol.* **1982**, *156*, 345−357.
(11) Maillard, D.; Prud'homme, R. E. *Macromolecules* **2006**, *39*, 4272−4275.
(12) Ray, S. S.; Okamoto, M. *Macromol. Rapid Commun.* **2003**, *24*, 815−840.
(13) Puiggali, J.; Ikada, Y.; Tsuji, H.; Cartier, L.; Okihara, T.; Lotz, B. *Polymer* **2000**, *41*, 8921−8930.
(14) Sasaki, S.; Asakura, T. *Macromolecules* **2003**, *36*, 8385−8390.
(15) Kikkawa, Y.; Abe, H.; Fujita, M.; Iwata, T.; Inoue, Y.; Doi, Y. *Biomacromolecules* **2001**, *2*, 940−945.
(16) Schultz, J. M. *Polymer Crystallization: The Development of Crystalline Order in Thermoplastic Polymers*; Oxford University Press: New York, 2001.
(17) Reiter, G.; Sommer, J.-U. *Polymer Crystallization: Observations, Concepts and Interpretations*; Springer: Berlin, 2003.
(18) Sarasua, J. R.; Lopez, N. R.; Arraiza, A. L.; Meaurio, E. *Macromolecules* **2005**, *38*, 8362−8371.
(19) Xu, J.; Guo, B.; Zhou, J.; Li, L.; Wu, J.; Kowalczuk, M. *Polymer* **2005**, *46*, 9176−9185.
(20) Céré, F. M.Sc. Thesis, Département de Chimie, Université de Montréal, Montréal, 2006; p 78.
(21) Kikkawa, Y.; Abe, H.; Iwata, T.; Inoue, Y.; Doi, Y. *Biomacromolecules* **2002**, *3*, 350−356.
(22) Li, C. Y.; Cheng, S. Z. D.; Weng, X.; Ge, J. J.; Bai, F.; Zhang, J. Z.; Calhoum, B. H.; Harris, F. W.; Chien, L.; Lotz, B. *J. Am. Chem. Soc.* **2001**, *123*, 2462−2463.
(23) Oaki, Y.; Imai, H. *Langmuir* **2007**, *23*, 5466−5470.
(24) Nandi, N.; Vollhardt, D. *Chem. Rev.* **2003**, *103*, 4033−4076.
(25) Li, C. Y.; Cheng, S. Z. D.; Ge, J. J.; Bai, F.; Zhang, J. Z.; Mann, I. K.; Harris, F. W.; Chien, L.; Yan, D.; He, T.; Lotz, B. *Phys. Rev. Lett.* **1999**, *83*, 4558−4561.
(26) Li, C. Y.; Ge, J. J.; Bai, F.; Calhoum, B. H.; Harris, F. W.; Cheng, S. Z. D.; Chien, L.; Lotz, B.; Keith, H. D. *Macromolecules* **2001**, *34*, 3634−3641.
(27) Li, C. Y.; Jin, S.; Weng, X.; Ge, J. J.; Zhang, D.; Bai, F.; Harris, F. W.; Cheng, S. Z. D.; Yan, D.; He, T.; Lotz, B.; Chien, L. *Macromolecules* **2002**, *35*, 5475−5482.

MA071306U